

Gravity-induced transparency

Yongjie Pan and Baocheng Zhang*

School of Mathematics and Physics, China University of Geosciences, Wuhan 430074, China

We investigate the transition amplitudes of the Unruh-DeWitt detector within the Schwarzschild spacetime background and discover gravity-induced transparency phenomena akin to the earlier acceleration-induced transparency. This is confirmed through calculations performed in both the Hartle-Hawking and Unruh states. The similarity between free-falling detectors in these states and accelerated detectors in electromagnetic fields is noteworthy, as it parallels the scenario in which acceleration-induced transparency phenomena occur.

I. INTRODUCTION

Acceleration-induced phenomena have garnered significant attention in physics research. Notable examples include the Unruh effect [1], the anti-Unruh effect [2, 3], and acceleration-induced transparency (AIT) phenomena [4]. While the former two effects have been extensively studied theoretically, the AIT phenomenon holds particular experimental significance. As is well-known, detecting the Unruh effect experimentally presents challenges due to the exceedingly low Unruh temperature; for instance, achieving a thermal bath at 1 K would require an acceleration of 10^{20} m/s². Recent work on AIT has proposed a method to amplify the Unruh effect by subjecting the Unruh-DeWitt (UDW) detector to acceleration within an electromagnetic field rather than in vacuum. For the Fock state, the Unruh effect is enhanced by a factor of $n + 1$ (where n is the photon number) compared to the scenario occurring in vacuum. Additionally, it has been found that the anti-Unruh effect can also be amplified through a simulated light-matter interaction akin to the AIT phenomenon [5].

Given that the equivalence principle links the Unruh effect to the Hawking effect [6], and considering the challenge in detecting Hawking radiation, it is pertinent to explore whether the AIT effect can be extended to its gravity-induced analogue. Hawking radiation can be likened to the electromagnetic field, while a detector near a Schwarzschild black hole mirrors an accelerated detector in flat spacetime. Consequently, it seems feasible to obtain gravity-induced transparency phenomena for a detector near a black hole. However, a hurdle arises in obtaining analytic expressions for field mode solutions [7, 8] when calculating field mode solutions in (3+1)-dimensional Schwarzschild spacetime. Despite this, the transition rate of a detector near a black hole has been studied previously in various scenarios, including static detectors near Schwarzschild black holes [7], the anti-Hawking effect for BTZ black holes [9], rotating BTZ black holes [10], and free-fall detectors near black holes [11]. Hence, it is possible to apply the methodologies from these studies to investigate gravity-induced trans-

parency phenomena for a UDW detector moving outside a Schwarzschild black hole.

This paper is organized as follows. In Sec. II, we present a model for the interaction between detectors and fields in flat spacetime and extend the definition of AIT phenomena. Sec. III is devoted to the investigation of gravity-induced transparency phenomena for a free-falling detector in the exterior region of a black hole. Finally, we summarize and give the conclusion in Sec. IV.

II. THE INTERACTION MODEL

We start with the model of the UDW detector, commonly regarded as a pointlike two-level quantum system. The interaction Hamiltonian is expressed as [12, 13]

$$H_I = \lambda \chi(\tau) \mu(\tau) \phi[x(\tau), t(\tau)], \quad (1)$$

where λ is the coupling constant between the accelerated detector and the scalar field, $\mu(\tau) = e^{i\Omega\tau} \sigma^+ + e^{-i\Omega\tau} \sigma^-$ represents the detector's monopole moment with σ^\pm being SU(2) ladder operators. The detector possesses two distinct energy levels denoted by the ground $|g\rangle$ and excited $|e\rangle$ states, respectively, separated by an energy gap Ω in the detector's rest frame. $\phi[x(\tau), t(\tau)]$ is the field operator in which $x(\tau), t(\tau)$ represents the detector's trajectory, and $\chi(\tau)$ is the switching function. For the purposes of this paper, we set $\chi(\tau)$ to be equal to 1.

The time evolution operator under the Hamiltonian (1) is obtained through the following perturbative expansion to the first order

$$\begin{aligned} U &= 1 - i \int d\tau H_I(\tau) + \mathcal{O}(\lambda^2) \\ &= 1 - i\lambda \sum_k [\eta_k^+ a_k^\dagger \sigma^\dagger + \eta_k^- a_k \sigma^\dagger + H.c.]. \end{aligned} \quad (2)$$

In the quantum description of light-matter interaction, $a_k^\dagger \sigma^\dagger$ and $a_k \sigma^-$ are the counter-rotating wave terms, while $a_k \sigma^\dagger$ and $a_k^\dagger \sigma^-$ are the rotating wave terms. \sum_k represents the summation of all momentum modes in the field. $\eta_k^\pm = \int \frac{\lambda d\tau}{\sqrt{(2\pi)^3 2\omega}} e^{i\Omega\tau \pm ik^\mu x_\mu}$ where $k^\mu x_\mu = \omega t(\tau) - kx(\tau)$ are related to the trajectory of the detector. a_k^\dagger and a_k are the creation and annihilation operators for the field

*Electronic address: zhangbaocheng@cug.edu.cn

ϕ which can be expressed as $\hat{\phi}(x) = \int dk(u_k \hat{a}_k + H.c.)$ where $u_k = [2\omega(2\pi)]^{-1/2} e^{-ik_\mu x^\mu}$.

In the interaction picture, this evolution is described by

$$U|g\rangle|n\rangle_k = |g\rangle|n\rangle_k - i\sqrt{n}\eta_-|e\rangle|n-1\rangle_k - i\sqrt{n+1}\eta_+|e\rangle|n+1\rangle_k, \quad (3)$$

$$U|e\rangle|n\rangle_k = |e\rangle|n\rangle_k - i\sqrt{n+1}\eta_-^*|g\rangle|n+1\rangle_k - i\sqrt{n}\eta_+^*|g\rangle|n-1\rangle_k. \quad (4)$$

where $|n\rangle_k$ is the Fock state of the field indicating the presence of n photons in the k mode. In the equations (3) and (4), the second and third terms on the right side represent the rotating-wave and counter-rotating-wave terms, respectively. For instance, the second term in Eq. (3) signifies the absorption of energy by the detector from the field, causing a transition from the ground state to the excited state, commonly referred to as the stimulated absorption term [4, 5]. The third term in Eq. (3) accounts for the contribution of the Unruh effect, arising from the accelerated motion of the detector within the photon field, known as the stimulated Unruh effect term. Equation (4) can be interpreted similarly.

At first, we consider the field to be in the vacuum where $n_k = 0$ for any k mode. When the detector is accelerated in the vacuum state with the trajectory [14, 15]

$$x^\mu(\tau) = [\sinh(a\tau)/a, \cosh(a\tau)/a], \quad (5)$$

we have the transition probability, which is proportional to

$$|\eta^+|^2 = \lambda^2 \frac{2\pi/(\Omega a)}{e^{\Omega/(k_B T_U)} - 1}. \quad (6)$$

This corresponds to a Bose-Einstein distribution at a temperature $T_U = \frac{a}{2\pi}$. This implies that the conventional Unruh effect [1, 16], which arises from a uniformly accelerating motion of the detector in vacuum, is equivalent to the detector being immersed in a thermal bath at a temperature of T_U .

When we replace the vacuum field state with a single-mode Fock state $|n\rangle$, we obtain the transition probability

$$P \propto (n+1)|\eta_+|^2. \quad (7)$$

It is evident that the transition probability of the detector is amplified by a factor of $(n+1)$. This amplification could bring the transition probability of the detector into an experimentally observable range, thereby facilitating the experimental observation of the Unruh effect. Achieving this has been challenging in previous studies [17].

As electromagnetically induced transparency [18] refers to the suppression of the rotating-wave term in the model of light-matter interaction (the counter-rotating wave term is neglected due to its violation of the conservation of energy), the AIT phenomenon presents a similar

mechanism. In AIT, the rotating-wave term in the interaction between the detector and the field is suppressed, while the counter-rotating wave term contributes to the transition of the detector. This can be expressed mathematically as the condition that $\frac{|\eta_-|}{|\eta_+|} \ll 1$.

III. GRAVITY-INDUCED TRANSPARENCY

Now we turn to the situation of the curved spacetime and examine the behaviors of the detector in the vicinity of a Schwarzschild black hole, characterized by the metric

$$ds^2 = -\left(1 - \frac{2M}{r}\right) dt^2 + \left(1 - \frac{2M}{r}\right)^{-1} dr^2 + r^2(d\theta^2 + \sin^2\theta d\phi^2), \quad (8)$$

where $M > 0$ is the mass of the black hole.

To investigate the interaction between a UDW detector and the field within the framework of Schwarzschild spacetime (8), and to compute the transition amplitude of the detector, the vacuum states are required. In this paper, we will perform calculations using two distinct field states: the Hartle-Hawking state [19] and the Unruh state [1].

We begin by considering the free-falling process of the detector, commencing at a distance R from the center of the black hole. The initial state of the field is denoted by $|n\rangle_S$, where S distinguishes between the two different field states. Following the interaction between the detector and the field, we derive the transition amplitude of the detector as

$$\eta_S^\pm = \int d\tau e^{i\Omega\tau} \langle n \pm 1 |_S \phi_S(\tau) |n\rangle_S. \quad (9)$$

This “+” term corresponds to the counter-rotating wave term, signifying the emission of photons from the field when the detector transitions from the ground state to the excited state. Conversely, the “-” term corresponds to the rotating-wave term, representing the process in which the detector absorbs the energy of a photon from the field while transitioning from the ground state to the excited state.

In order to calculate the transition amplitude (9), we have to solve the field ϕ_S . Mode solutions of the Klein-Gordon equation in the Schwarzschild spacetime have the form:

$$u = \frac{1}{\sqrt{4\pi\omega}} r^{-1} \rho_{\omega\ell}(r) Y_{\ell m}(\theta, \phi) e^{-i\omega t}, \quad (10)$$

where $\omega > 0$, $Y_{\ell m}$ is the spherical harmonic function and the radial function $\rho_{\omega\ell}$ satisfies

$$\frac{d^2 \rho_{\omega\ell}}{dr^{*2}} + \left\{ \omega^2 - \left(1 - \frac{2M}{r}\right) \left[\frac{\ell(\ell+1)}{r^2} + \frac{2M}{r^3} \right] \right\} \rho_{\omega\ell} = 0, \quad (11)$$

with r^* being the tortoise coordinate defined as $r^* = r + 2M \log(r/2M - 1)$. When $r \rightarrow \infty$, the radial function can be solved as

$$\rho_{\omega\ell}^{r \rightarrow \infty} = e^{\pm i\omega r^*}. \quad (12)$$

However, analytical solutions are not available at any finite radial position, necessitating the use of numerical solutions. From the asymptotic forms in Eq. (12), two types of field modes can be classified. One type is the “up-modes” associated with mode solutions exhibiting the leading-order form $e^{+i\omega r^*}$ at infinity. The other type is the “in-modes” associated with mode solutions exhibiting the leading-order form $e^{-i\omega r^*}$ at infinity.

As outlined in Ref. [7] (also refer to Appendix A for comprehensive calculation details), it is crucial to handle the radial function with care. This is because the radial functions solved from Eq. (11) cannot be directly substituted into the mode solution in Eq. (10) due to the differing boundary conditions of the two modes.

In the exterior region of the Schwarzschild black hole, a complete set of normalized basis functions for the massless scalar field is given by [20, 21]

$$\begin{aligned} u_{\omega\ell m}^{in}(x) &= \frac{1}{\sqrt{4\pi\omega}} \Phi_{\omega\ell}^{in}(r) Y_{\ell m}(\theta, \phi) e^{-i\omega t}, \\ u_{\omega\ell m}^{up}(x) &= \frac{1}{\sqrt{4\pi\omega}} \Phi_{\omega\ell}^{up}(r) Y_{\ell m}(\theta, \phi) e^{-i\omega t}. \end{aligned} \quad (13)$$

In this context, the radial function $\psi_{\omega\ell}(r) = \rho_{\omega\ell}(r)/r$ of the mode solution in Eq. (10) is normalized to yield the normalized function $\Phi_{\omega\ell}(r)$. Utilizing the bases $u_{\omega\ell m}^{in}(x)$ and $u_{\omega\ell m}^{up}(x)$, the quantum field can be expressed for the vacuum states within the black hole spacetime. Further details can be found in the Appendix B.

The further calculation necessitates the determination of the detector’s geodesics, which remains the same for the two distinct vacuum states. We consider the detector initiating its free-fall at a distance R from the black hole, with the geodesics given as [22]

$$\left(\frac{dr}{d\tau}\right)^2 = \frac{2M}{r} - (1 - E^2), \quad \frac{dt}{d\tau} = \frac{E}{1 - 2M/r}. \quad (14)$$

where $E^2 = 1 - 2M/R$ is related to the initial position R . In this paper, we consider a finite free-falling distance ΔR for the detector.

Firstly, we calculate the transition amplitude for the Hartle-Hawking vacuum state. The Hartle-Hawking vacuum state $|0\rangle_H$ is defined over the entire spacetime and represents a state in which the black hole and its surroundings are in thermal equilibrium at the same temperature as that of the black hole [19, 23].

In order to calculate the transition amplitude in the Hartle-Hawking state, we must expand the quantum field

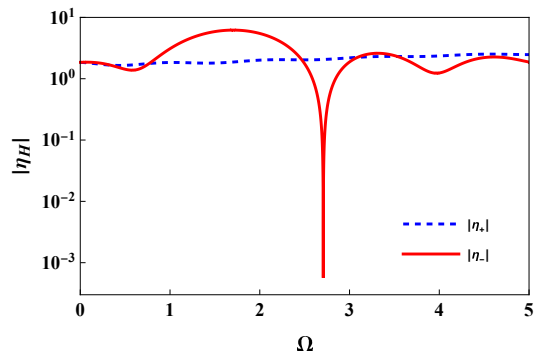


FIG. 1: The transition amplitude as a function of the atomic energy gap for the Hartle-Hawking state. The red solid line denotes the process in which the detector absorbs a photon from the field and then jumps from the ground state to the excited state, and the blue dashed line denotes the process in which the field excites a photon while the detector jumps to the excited state.

in terms

$$\begin{aligned} w_{\omega\ell m}^{in} &= \frac{1}{\sqrt{2 \sinh(4\pi M\omega)}} (e^{2\pi M\omega} u_{\omega\ell m}^{in} + e^{-2\pi M\omega} v_{\omega\ell m}^{in*}), \\ \bar{w}_{\omega\ell m}^{in} &= \frac{1}{\sqrt{2 \sinh(4\pi M\omega)}} (e^{-2\pi M\omega} u_{\omega\ell m}^{in*} + e^{2\pi M\omega} v_{\omega\ell m}^{in}), \\ w_{\omega\ell m}^{up} &= \frac{1}{\sqrt{2 \sinh(4\pi M\omega)}} (e^{2\pi M\omega} u_{\omega\ell m}^{up} + e^{-2\pi M\omega} v_{\omega\ell m}^{up*}), \\ \bar{w}_{\omega\ell m}^{up} &= \frac{1}{\sqrt{2 \sinh(4\pi M\omega)}} (e^{-2\pi M\omega} u_{\omega\ell m}^{up*} + e^{2\pi M\omega} v_{\omega\ell m}^{up}). \end{aligned} \quad (15)$$

In the exterior region of the black hole, the v functions vanish. With these terms, we can expand the field as

$$\begin{aligned} \phi_H &= \sum_{\ell=0}^{\infty} \sum_{m=-\ell}^{+\ell} \int_0^{\infty} d\omega (d_{\omega\ell m}^{up} w_{\omega\ell m}^{up} + \bar{d}_{\omega\ell m}^{up} \bar{w}_{\omega\ell m}^{up} \\ &\quad + d_{\omega\ell m}^{in} w_{\omega\ell m}^{in} + \bar{d}_{\omega\ell m}^{in} \bar{w}_{\omega\ell m}^{in} + H.c.) \end{aligned} \quad (16)$$

where d^j and \bar{d}^j are the annihilation operators, and satisfy

$$d_{\omega\ell m}^j |0\rangle_H = \bar{d}_{\omega\ell m}^j |0\rangle_H = 0. \quad (17)$$

where $j \in \{in, up\}$. $H.c.$ represents the Hermitian conjugate terms and $d^{j\dagger}$ and $\bar{d}^{j\dagger}$ are the corresponding creation operators.

Upon substituting the field ϕ_H into the Eqs. (9) (see the Appendix C for the detailed calculation), we derive the transition amplitude of the detector, as depicted in Fig. 1. The figure vividly illustrates the variation of the transition amplitude. Notably, a distinct absorption phenomenon emerges for a specific energy gap, resembling the behavior observed in AIT. This observation indicates the presence of gravity-induced transparency within the Schwarzschild spacetime for the Hartle-Hawking state.

In contrast to the Hartle-Hawking state, which arises from the idealization of time symmetry, the Unruh vacuum state is associated with a realistic black hole formed

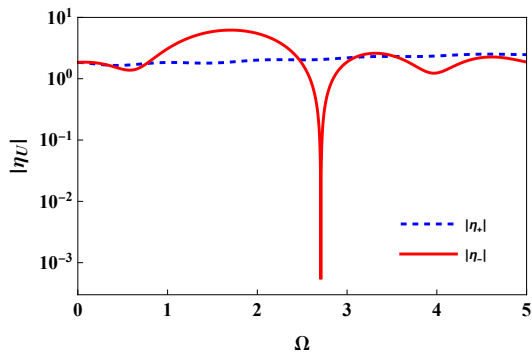


FIG. 2: Transition amplitude of the detector for the Unruh state. The lines in this figure have the same meaning as that in Fig. 1.

via collapse and emerges from the inquiry into the reality of black hole radiation. Consequently, the Unruh state is not applicable to the in-modes originating from past infinity. Then, we can expand the field

$$\begin{aligned} \phi_U = & \sum_{\ell=0}^{\infty} \sum_{m=-\ell}^{+\ell} \int_0^{\infty} d\omega (d_{\omega\ell m}^{up} w_{\omega\ell m}^{up} + \bar{d}_{\omega\ell m}^{up} \bar{w}_{\omega\ell m}^{up} \\ & + b_{\omega\ell m}^{in} u_{\omega\ell m}^{in} + H.c.), \end{aligned} \quad (18)$$

where $b_{\omega\ell m}^{in} |0\rangle_U = d_{\omega\ell m}^{up} |0\rangle_U = \bar{d}_{\omega\ell m}^{up} |0\rangle_U = 0$.

Similar to the calculation for the Hartle-Hawking state, we can obtain the results of the gravity-induced transparency phenomenon in the Unruh state, as illustrated in Fig. 2. It is found that the energy gap required for the emergence of gravity-induced transparency is essentially the same as that in the Hartle-Hawking state. This similarity arises from the fact that the field types used in defining the Unruh and Hartle-Hawking states are fundamentally alike. For both the Unruh state and the Hartle-Hawking state, the transition rates of the detector are proportional to $\frac{1}{2E(e^{E/kT}-1)}$ and $\frac{1}{E(e^{E/kT}-1)}$, respectively [24], differing only by a constant factor of 1/2. Hence, the change in the transition amplitude with the energy gap of the detector also yields essentially the same results.

Finally, it's worth emphasizing that the Boulware vacuum state [25] is not suitable for our study. This is because no Hawking radiation exists relative to the Boulware vacuum for the free-falling observers. In particular, the Boulware vacuum is not employed for the free-falling observers due to the divergence of the energy-momentum tensor at the horizon of the black hole [24].

IV. CONCLUSION

In this paper, we employ numerical methods to investigate a detector coupled to a massless scalar field in both the Hartle-Hawking and Unruh states. We compute the transition amplitudes of the detector in these two states and identify gravity-induced transparency phenomena,

akin to AIT phenomena observed for an accelerated detector in an electromagnetic field. Notably, we find that the energy gap of the detector remains consistent between the two states when gravity-induced transparency occurs. This consistency arises from the nearly identical definitions of field modes in these two states for our purpose. Extending our study to other black hole spacetimes presents an intriguing avenue for future research.

V. ACKNOWLEDGMENTS

This work is supported by National Natural Science Foundation of China (NSFC) with Grant No. 12375057 and the Fundamental Research Funds for the Central Universities, China University of Geosciences (Wuhan).

Appendix A: Radial Function $\rho_{\omega\ell}$

To solve the differential equation in Eq. (11) of the main text, we introduce the function

$$\psi_{\omega\ell}(r) := \rho_{\omega\ell}(r)/r, \quad (A1)$$

which satisfies:

$$\begin{aligned} \psi_{\omega\ell}''(r) + \frac{2(r-M)}{r(r-2M)} \psi_{\omega\ell}'(r) \\ + \left(\frac{\omega^2 r^2}{(r-2M)^2} - \frac{\xi}{r(r-2M)} \right) \psi_{\omega\ell}(r) = 0, \end{aligned} \quad (A2)$$

with $\xi = \ell(\ell+1)$.

For the up-modes, to numerically obtain their value at a given suitably large radius r_{∞} , we substitute the ansatz

$$\psi_{a\ell}^{up} \sim \frac{e^{iar^*}}{r} e^{v(r)}, \quad v(r) := \sum_{n=1}^{\infty} \frac{c_n}{r^n}, \quad (A3)$$

into Eq. (A2) and leads to an equation for $v(r)$,

$$\begin{aligned} r^2(r-2M)v''(r) + r^2(r-2M)(v'(r))^2 \\ + 2r(M+i\omega r^2)v'(r) - (\ell(\ell+1)r+2M) = 0. \end{aligned} \quad (A4)$$

Then, we substitute the expression of $v(r)$ in Eq. (A3) into Eq. (A4) and collect inverse powers of r . The coefficient of each power of r must be set equal to zero. In practice, the upper limit in the sum (A3) is replaced by some suitable cutoff, denoted as n_{∞} .

The initial conditions for the up-modes are taken as

$$\begin{aligned} \psi_{\omega\ell}^{up}(r_{\infty}) &= \frac{e^{i\omega r^*(r_{\infty})}}{r_{\infty}} e^{v(r_{\infty})}, \\ \psi_{a\ell}^{up'}(r_{\infty}) &= \frac{d}{dr} \left[\frac{e^{i\omega r^*(r)} e^{v(r)}}{r} \right]_{r=r_{\infty}}. \end{aligned} \quad (A5)$$

These conditions would become more accurate as n_{∞} and r_{∞} take larger values. We use the initial conditions

(A5) to make the calculation and take the parameters as $n_\infty = 100$ and $r_\infty = 15000M$, and thus we can obtain a numerical solution for $\psi_{\omega\ell}^{up}(r)$.

For the in-modes, we have

$$\psi_{\omega\ell}^{in} \sim \frac{e^{-i\omega r^*}}{r} w(r), \quad w(r) := \sum_{n=0}^{\infty} b_n (r - 2M)^n. \quad (\text{A6})$$

Similarly, we substitute Eq. (A6) into Eq. (A2) to obtain an equation about $w(r)$ as

$$r^2(r - 2M)w''(r) + 2r(M - ir^2\omega)w'(r) - (\ell(\ell + 1)r + 2M)w(r) = 0. \quad (\text{A7})$$

According to Eq. (A6) and (A7), we can get

$$\begin{aligned} b_0 &= 1, \quad b_{-1} = b_{-2} = 0, \\ b_n &= \frac{-[-12i\omega M(n-1) + (2n-3)(n-1) - (\ell(\ell+1) + 1)]}{2M(n^2 - i4Mn\omega)} b_{n-1} \\ &\quad - \frac{[(n-2)(n-3) - i12M\omega(n-2) - \ell(\ell+1)]}{4M^2(n^2 - i4Mn\omega)} b_{n-2} \\ &\quad + \frac{i\omega(n-3)}{2M^2(n^2 - i4Mn\omega)} b_{n-3}. \end{aligned}$$

The initial conditions for the in-modes are taken as

$$\begin{aligned} \psi_{\omega\ell}^{in}(r_H) &= \frac{e^{-i\omega r^*}(r_H)}{r_H} w(r_H), \\ \psi_{\omega\ell}^{in'}(r_H) &= \frac{d}{dr} \left[\frac{e^{-i\omega r^*}(r)}{r} w(r) \right]_{r=r_H}. \end{aligned} \quad (\text{A8})$$

We use the initial conditions (A8) to make the calculation and take the parameters as $n_\infty = 200$ and $r_H = 2.0000001M$, and thus we can obtain a numerical solution for $\psi_{\omega\ell}^{in}(r)$.

The numerical results for $\psi_{\omega\ell}^{up}(r)$ and $\psi_{\omega\ell}^{in}(r)$ can be used to calculate the transition amplitude of the detector in the curved spacetime.

Appendix B: Normalisation

In this section we deal with the normalization of radial functions for the mode solution in Eq. (10) of the main text.

We choose radial function Ψ satisfies the following asymptotic form

$$\begin{aligned} \Psi_{\omega\ell}^{in}(r) &\sim \begin{cases} B_{\omega\ell}^{in} e^{-i\omega r^*}, & r \rightarrow 2M, \\ r^{-1} e^{-i\omega r^*} + A_{\omega\ell}^{in} r^{-1} e^{+i\omega r^*}, & r \rightarrow \infty, \end{cases} \\ \Psi_{\omega\ell}^{up}(r) &\sim \begin{cases} A_{\omega\ell}^{up} e^{-i\omega r^*} + e^{+i\omega r^*}, & r \rightarrow 2M, \\ B_{\omega\ell}^{up} r^{-1} e^{+i\omega r^*}, & r \rightarrow \infty. \end{cases} \end{aligned} \quad (\text{B1})$$

and $A_{\omega\ell}^{up}, B_{\omega\ell}^{up}$ are the transmission and reflection coefficients that satisfy the following Wronskian relations

$$\begin{aligned} B_{\omega\ell}^{up} &= \frac{(2M)2i\omega}{W[\rho_{\omega\ell}^{in}, \rho_{\omega\ell}^{up}]}, \quad A_{\omega\ell}^{up} = -\frac{W[\rho_{\omega\ell}^{in}, \rho_{\omega\ell}^{up}]^*}{W[\rho_{\omega\ell}^{in}, \rho_{\omega\ell}^{up}]}, \\ A_{\omega\ell}^{in} &= -\frac{W[\rho_{\omega\ell}^{in}, \rho_{\omega\ell}^{up*}]}{W[\rho_{\omega\ell}^{in}, \rho_{\omega\ell}^{up}]}. \end{aligned} \quad (\text{B2})$$

We replace the function $\Psi_{\omega\ell}^j(r)$ with $F_{\omega\ell}^j(r)$, $j \in \{in, up\}$, defined by

$$F_{\omega\ell}^{in} = \Psi_{\omega\ell}^{in}, \quad F_{\omega\ell}^{up} = \frac{\Psi_{\omega\ell}^{up}}{2M}. \quad (\text{B3})$$

It can be verified that the functions $R_{\omega\ell}^j(r) := rF_{\omega\ell}^j(r)$ are normalized, with the relationship between reflection and transmission coefficients

$$\begin{aligned} B_{all}^{up} &= (2M)^2 B_{all}^{in}, \quad |A_{\omega\ell}^{in}|^2 = 1 - 4M^2 |B_{\omega\ell}^{in}|^2, \\ |A_{al}^{in}|^2 &= |A_{al}^{up}|^2, \quad |A_{al}^{up}|^2 = 1 - \frac{|B_{\omega\ell}^{up}|^2}{4M^2}. \end{aligned} \quad (\text{B4})$$

Then, we can define

$$\begin{aligned} \Phi_{\omega\ell}^{in}(r) &= \frac{B_{\omega\ell}^{up} \psi_{\omega\ell}^{in}(r)}{2M}, \\ \Phi_{\omega\ell}^{up}(r) &= \frac{B_{\omega\ell}^{up} \psi_{\omega\ell}^{up}(r)}{2M}. \end{aligned} \quad (\text{B5})$$

Using the Eq. (B4), it can be shown that the solution in Eq. (13) of the main text satisfies the orthogonal normalization relation as follows

$$\begin{aligned} (u_{\omega\ell m}^{up}, u_{\omega'\ell' m'}^{up}) &= \delta_{\ell\ell'} \delta_{mm'} \delta(\omega - \omega'), \\ (u_{\omega\ell m}^{in}, u_{\omega'\ell' m'}^{in}) &= \delta_{\ell\ell'} \delta_{mm'} \delta(\omega - \omega'), \\ (u_{\omega\ell m}^{in}, u_{\omega'\ell' m'}^{up}) &= 0, \end{aligned} \quad (\text{B6})$$

and the coefficient $B_{\omega\ell}^{up}$ can be obtained by substituting $\rho_{\omega\ell}^{up}$ and $\rho_{\omega\ell}^{in}$ into (B2).

Appendix C: Transition Amplitude

We consider free-falling process of the detector starting at the position R which is the distance from the center of the black hole.

For the Hartler-Hawking state, the transition amplitude is calculated as

$$\begin{aligned} \eta_H^+ &= \int d\tau e^{i\Omega\tau} \langle n+1 |_H \phi_H(\tau) |n\rangle_H \\ &= \int d\tau e^{i\Omega\tau} \langle n+1 |_H \sum_{\ell=0}^{\infty} \sum_{m=-\ell}^{+\ell} \int_0^{\infty} d\omega (d_{\omega\ell m}^{up} w_{\omega\ell m}^{up} \\ &\quad + \bar{d}_{\omega\ell m}^{up} \bar{w}_{\omega\ell m}^{up} + d_{\omega\ell m}^{in} w_{\omega\ell m}^{in} + \bar{d}_{\omega\ell m}^{in} \bar{w}_{\omega\ell m}^{in} + H.c.) |n\rangle_H \\ &= \int d\tau e^{i\Omega\tau} \sum_{\ell=0}^{\infty} \sum_{m=-\ell}^{+\ell} \int_0^{\infty} d\omega \\ &\quad (w_{\omega\ell m}^{up*} + \bar{w}_{\omega\ell m}^{up*} + w_{\omega\ell m}^{in*} + \bar{w}_{\omega\ell m}^{in*}) \\ &= f_1 + f_2 + f_3 + f_4. \end{aligned} \quad (\text{C1})$$

Note that the integration over field frequencies will vanish when we only consider a single field frequency. The above equation is divided into four terms and their calculation

process is similar. Here, we take the calculation process for f_1 as an example,

$$\begin{aligned}
f_1 &= \int d\tau e^{i\Omega\tau} \sum_{\ell=0}^{\infty} \sum_{m=-\ell}^{+\ell} (w_{\omega\ell m}^{up*}) \\
&= \int d\tau e^{i\Omega\tau} \sum_{\ell=0}^{\infty} \sum_{m=-\ell}^{+\ell} \frac{1}{\sqrt{2 \sinh(4\pi\omega M)}} (e^{2\pi M\omega} u_{\omega\ell m}^{up*}) \\
&= \int d\tau e^{i\Omega\tau} \sum_{\ell=0}^{\infty} \sum_{m=-\ell}^{+\ell} \frac{e^{2\pi\omega M} Y_{\ell m}^*(\theta, \beta) e^{i\omega t}}{\sqrt{8\pi\omega \sinh(4\pi M\omega)}} \Phi_{\omega\ell}^{up*}(r) \\
&= \int d\tau e^{i\Omega\tau} \sum_{\ell=0}^{\infty} \sum_{m=-\ell}^{+\ell} \frac{e^{2\pi\omega M} Y_{\ell m}^*(\theta, \beta) e^{i\omega t}}{\sqrt{8\pi\omega \sinh(4\pi M\omega)}} \frac{B_{\omega\ell}^{up} \psi_{\omega\ell}^{up*}(r)}{2M} \quad (C2)
\end{aligned}$$

For a detector that starts its free fall at R , we cannot obtain a precise expression for the world line $r(\tau), t(\tau)$ from Eq. (14) of the main text. So we can't just substitute this world line into the field $\phi_S[t(\tau), r(\tau)]$. We require to make the transformation to obtain the geodesics,

$$\begin{aligned}
d\tau &= \frac{dr}{\sqrt{\frac{2M}{r} - (1 - E^2)}}, \\
dt &= \frac{E}{1 - 2M/r} \frac{dr}{\sqrt{\frac{2M}{r} - (1 - E^2)}}. \quad (C3)
\end{aligned}$$

In particular, $E = 1$ when the detector starts its free fall from infinity $R = \infty$. For our purpose, the detector starts its free fall from $2M < R = \text{Constant}$. Make the integral in Eq. (C3) to obtain,

$$\begin{aligned}
\tau(r) &= \frac{\sqrt{-1 + E^2 + \frac{2M}{r}}}{-1 + E^2} - \frac{2M \tan^{-1} \left[\frac{\sqrt{-1 + E^2 + \frac{2M}{r}}}{\sqrt{1 - E^2}} \right]}{(1 - E^2)^{3/2}}, \\
t(r) &= \frac{E \sqrt{-1 + E^2 + \frac{2M}{r}}}{-1 + E^2} - 4M \tanh^{-1} \left[\frac{\sqrt{-1 + E^2 + \frac{2M}{r}}}{E} \right] \\
&\quad + E \frac{2(-3 + 2E^2) M \tan^{-1} \left[\frac{\sqrt{-1 + E^2 + \frac{2M}{r}}}{\sqrt{1 - E^2}} \right]}{(1 - E^2)^{3/2}} \quad (C4)
\end{aligned}$$

Then, the function f_1 becomes

$$\begin{aligned}
f_1 &= \int_{R-\Delta R}^R dr \sum_{\ell=0}^{\infty} \sum_{m=-\ell}^{+\ell} \frac{e^{i\Omega\tau(r)}}{\sqrt{\frac{2M}{r} - \frac{2M}{R}}} \\
&\quad \times \frac{e^{2\pi\omega M} Y_{\ell m}^*(\theta, \beta) e^{i\omega t(r)}}{\sqrt{8\pi\omega \sinh(4\pi M\omega)}} \frac{B_{\omega\ell}^{up} \psi_{\omega\ell}^{up*}(r)}{2M}, \quad (C5)
\end{aligned}$$

where ΔR is the free-falling distance for the detector. To get around the divergence caused by the term $1/(\sqrt{2M/r} - 2M/R)$, we change the integral over R into the form of a discrete point summation and remove the initial point. Thus, we get

$$\begin{aligned}
f_1 &= \sum_{n=0}^{n=N} \sum_{\ell=0}^{\infty} \sum_{m=-\ell}^{+\ell} \frac{e^{i\Omega\tau(r_n)}}{\sqrt{\frac{2M}{r_n} - \frac{2M}{R}}} \\
&\quad \times \frac{e^{2\pi\omega M} Y_{\ell m}^*(\theta, \beta) e^{i\omega t(r_n)}}{\sqrt{8\pi\omega \sinh(4\pi M\omega)}} \frac{B_{\omega\ell}^{up} \psi_{\omega\ell}^{up*}(r_n)}{2M}, \quad (C6)
\end{aligned}$$

where r_n denotes the n -th value in the $r_n \in \{R - \Delta R, R - \varepsilon\}$ interval up to N points. In the concrete calculation, we take the cutoff of ℓ to be $\ell = 5$, and the parameters $N = 20$, $R = 4.0029299M$, $\Delta R = 1.0029299M$, $\varepsilon = 0.0029299$.

The remaining three terms, f_2, f_3, f_4 , have a similar calculation. And the transition amplification in Eq. (9) of the main text for the Unruh vacuum state is calculated in the same way as η_H^+ .

-
- [1] W. G. Unruh, Notes on black-hole evaporation, Phys. Rev. D **14**, 870 (1976).
[2] W. G. Brenna, R. B. Mann, and E. Martín-Martínez, Anti-Unruh phenomena, Phys. Lett. B **757**, 307 (2016).
[3] L. J. Garay, E. Martín-Martínez, and J. De Ramón, Thermalization of particle detectors: The Unruh effect and its reverse, Phys. Rev. D **94**, 104048 (2016).
[4] B. Šoda, V. Sudhir, and A. Kempf, Acceleration-induced effects in stimulated light-matter interactions, Phys. Rev. Lett. **128**, 163603 (2022).
[5] Y. Pan and B. Zhang, Enhanced anti-Unruh effect by simulated light-matter interaction, Phys. Rev. D **107**, 085001 (2023).
[6] S. W. Hawking, Black hole explosions? Nature **248**, 30 (1974).
[7] L. Hodgkinson, J. Louko, and A. C. Ottewill, Static detectors and circular-geodesic detectors on the Schwarzschild black hole, Phys. Rev. D **89**, 104002 (2014).
[8] L. Hodgkinson, Particle detectors in curved spacetime quantum field theory, arXiv preprint arXiv:1309.7281 (2013).
[9] L. J. Henderson, R. A. Hennigar, R. B. Mann, A. R. Smith, and J. Zhang, Anti-hawking phenomena, Phys.

- Lett. B **809**, 135732 (2020).
- [10] M. P. Robbins and R. B. Mann, Anti-Hawking phenomena around a rotating BTZ black hole, *Phys. Rev. D* **106**, 045018 (2022).
- [11] M. O. Scully, S. Fulling, D. M. Lee, D. N. Page, W. P. Schleich, and A. A. Svidzinsky, Quantum optics approach to radiation from atoms falling into a black hole, *Proc. Natl. Acad. Sci. U.S.A.* **115**, 8131 (2018).
- [12] J. Louko and A. Satz, Transition rate of the Unruh-Dewitt detector in curved spacetime, *Class. Quantum Gravity* **25**, 055012 (2008).
- [13] B. S. DeWitt, Quantum gravity: the new synthesis, in *General Relativity* (1979).
- [14] L. C. Crispino, A. Higuchi, and G. E. Matsas, The Unruh effect and its applications, *Rev. Mod. Phys.* **80**, 787 (2008).
- [15] J. S. Ben-Benjamin, M. O. Scully, S. A. Fulling, D. M. Lee, D. N. Page, A. A. Svidzinsky, M. S. Zubairy, M. J. Duff, R. Glauber, W. P. Schleich, et al., Unruh acceleration radiation revisited, *Int. J. Mod. Phys. A* **34**, 1941005 (2019).
- [16] W. G. Unruh and R. M. Wald, What happens when an accelerating observer detects a Rindler particle, *Phys. Rev. D* **29**, 1047 (1984).
- [17] J. S. Bell and J. M. Leinaas, Electrons as accelerated thermometers, *Nucl. Phys. B* **212**, 131 (1983).
- [18] M. Fleischhauer, A. Imamoglu, and J. P. Marangos, Electromagnetically induced transparency: Optics in coherent media, *Rev. Mod. Phys.* **77**, 633 (2005).
- [19] J. B. Hartle and S. W. Hawking, Path-integral derivation of black-hole radiance, *Phys. Rev. D* **13**, 2188 (1976).
- [20] B. S. DeWitt, Quantum Field Theory in Curved Spacetime, *Phys. Rept.* **19**, 295-357 (1975)
- [21] P. Candelas, Vacuum polarization in Schwarzschild spacetime, *Phys. Rev. D* **21**, 2185 (1980).
- [22] S. Chandrasekhar and K. S. Thorne, *The mathematical theory of black holes*, (Oxford University Press, Oxford, UK, 1998).
- [23] W. Israel, Thermo-field dynamics of black holes, *Phys. Lett. A* **57**, 107 (1976).
- [24] N. D. Birrell and P. C. W. Davies, *Quantum fields in curved space*, (Cambridge University Press, Cambridge, UK, 1984).
- [25] D. G. Boulware, Quantum field theory in Schwarzschild and Rindler spaces, *Phys. Rev. D* **11**, 1404 (1975).